CONF 8710159--4

NUMERICAL SOLUTIONS OF TWO MOVING BOUNDARY PROBLEMS BY BOTH FINITE DIFFERENCE AND FINITE ELEMENT METHODS WITH APPLICATIONS

A. M. Hassanein
Argonne National Laboratory, Fusion Power Program

CONF-8710159--4

DE88 002867

1. ABSTRACT

The time dependent heat conduction equation is solved in different coordinate systems is solved subject to various boundary conditions. These boundary conditions include surface heat flux, energy to vaporization of target materials, radiation from surface to surrounding, and possible phase change of material. This system of equations is subject to two moving boundaries. One moving boundary being the melt-solid interface because the surface heat flux may result in melting the surface of the exposed material. Another moving boundary is the receding surface as a result of evaporation of the wall material due to the continuous heating of the melted surface. Both the finite difference and the finite element methods are used and compared in such solution to these problems. Physical applications to these problems include high energy deposition from electron or ion beams interaction with materials for space and weapons applications, plasma disruption and energy dump on the walls or components of a fusion reactor, and high energy laser welding and annealing of materials.

2. INTRODUCTION

Most moving boundary or Stefan problems (such as those discussed by Oziski [1], Muehlbauer and Sunderland [2] and in recent conferences [3,4]) deal with melting, solidification, or boiling, where the interface is mathematically characterized by a fixed value of the temperature. The present problem of intense evaporation involves a highly nonlinear boundary condition for the surface temperature whose determination is now an integral part of the solution for the entire problem.

Because of this added complication, previous treatments of intense evaporation were based on various simplifying assumptions regarding the condition at the moving boundary. Ready [5] assumed that evaporation begins and proceeds at a

constant boiling temperature when the laser pulse duration is large compared to the preheat time for reaching the boiling point. On the other hand, Ready [6] assumed for irradiations with Q-switched lasers that the vapor will be superheated to the critical point, and that the evaporation rate is determined by the thickness of material heated beyond the critical point.

Andrews and Atthey [7] developed a convenient analytical solution to the evaporation problem when it can be assumed that vaporization occurs at a constant boiling point. This solution has been used earlier by Loebel and Wolfer [8] to estimate the erosion by vaporization of various first wall materials. However, melting was neglected in this approach. Behrisch [9] has evaluated the evaporation due to heat pulses when the energy expended for both melting and evaporation is negligible compared to the total energy deposited.

FIRST HEADING HERE

All the above treatments avoid the central problem, namely that the rate of evaporation into a vacuum and the associated surface temperature are entirely determined by the kinetic processes involved in the vaporization, and by the energy partitioning between heat conductions, melting, evaporation, recondensation, and radiation.

Few attempts have been made to solve, in its entirety, this problem of evaporation into a vacuum. Csadin and Shapovalov [10] derived an integral equation for the surface temperature by neglecting melting and the receding motion of the evaporating surface. Golodenko and Kuz'michev [11] included the boundary motion in an approximate manner, but melting was again neglected, and constant thermophysical properties were assumed. Furthermore, no recondensation was included in any of the treatments.

More recently, several researchers [12-14] have carried out numerical studies on evaporation and melting during plasma disruptions, using similar models for evaporation as developed by the author [15-17].

In this paper however the numerical methods used in the solution of this two moving boundaries problem is discussed in detail, using both finite difference and finite element techniques. Several applications for this system of equations are also discussed. One application is due to intense energy deposition on the plasma chamber wall and its components in magnetic fusion devices. The energy deposited on part of the fusion reactor wall could exceed several hundred MJS with deposition times in the millisecond (ms) range or even shorter. The material behavior under this severe condition and the amount of material lost due to erosion from vaporization and melting is very important for the successful operation of a fusion reactor. Another application of this system of equa-

tions is to estimate the lifetime of reinjected small spherical pellets of solid material into the plasma edge to be vaporized and redeposited as coating or trapping material on part of the fusion reactor components.

3. FORMULATION OF THE PROBLEM

Although the above problem is solved in different coordinate systems such as one dimensional cartizian, one dimensional spherical, and two dimensional axially symmetric cylinderical coordinates, the discussions in this paper for simplicity will mainly be oriented towards the one dimensional cartizian coordinates. The general time-dependent one-dimensional heat conduction with thermophysical properties κ, ρ, C_p of the material vary with temperature is given by:

$$\rho_s(T)\, C_{p_s}(T) \frac{\partial T_s}{\partial t} = \frac{\partial}{\partial x}\left[K_s(T) \frac{\partial T_s}{\partial x}\right] \quad 0 < x < L,\ t > 0 \tag{1}$$

$$T(x,o) = f(x) \qquad 0 < x < L,\ t = 0 \tag{2}$$

where f(x) is the initial temperature distribution function. The developed computer code can also handle a volumetric heat generation source term Q(x,t) added to Eq. (1).

The correct boundary condition requires partitioning of the incident energy into conduction, melting, evaporation, and radiation. Thus the total input heat flux q(t):

$$q(t) = q_c + q_r + q_r \tag{3}$$

where

$$q_c = \text{conduction heat flux} = K(T) \left.\frac{\partial T}{\partial x}\right|_{x=0} \tag{4}$$

$$q_v = \text{vaporization heat flux} = \rho(T_v)\, L_v\, V(T_v) \tag{5}$$

$$q_r = \text{radiation heat flux} = \varepsilon\sigma\left(T_v^4 - T_a^4\right) \tag{6}$$

where $T_v = T(x = 0, t)$ is the surface temperature, L_v is the heat of vaporization, $v(T_v)$ is the velocity of the receding surface, σ is the Stefan-Boltzmann Constant, ε is the emissivity of the target material, and Ta is the ambient temperature of the surface not exposed to the energy dump but in direct line of sight of the exposed surface. Then the boundary condition at the surface can be written as

$$q(t) = -K(T)\frac{\partial T}{\partial x}\Big|_{x=0} + \text{Specified normal vapor heat} + \varepsilon\sigma\left(T_v^4 - T_a^4\right) \qquad (7)$$

Once melting commences, the condensed phases of the wall or target material define two regions (Fig. 1): $s(t) < x < m(t)$, and the solid phase in the region $x > m(t)$. Here, $m(t)$ is the instantaneous position of the melt-solid interface. The boundary condition at the melt-solid interface is now

$$k_s \frac{\partial T_s}{\partial x} - k_\ell \frac{\partial T_\ell}{\partial x} = \rho L_f w(t) \qquad \text{at } x = m(t) \qquad (8)$$

where

$$w(t) = \frac{dm}{dt} \ , \qquad (9)$$

is the velocity of the moving interface and L_f is the latent heat of fusion. The subscripts s and ℓ refer to solid and liquid phases respectively. The thermophysical properties of both solid and liquid phases are different and assumed to vary with temperatures by polonominal functions.

There are several ways of accounting for the moving boundary at the surface due to the evaporation of the wall material. One way is to introduce a coordinate frame which moves with the receding surface. Hence, in a frame

$$z(t) = x - \int_0^t v(T)\, dt \qquad (10)$$

The surface remains at $z=0$, but the heat conduction equation transforms into

$$\rho C_p \frac{\partial T}{\partial t} - \rho C_p v(T) \frac{\partial T}{\partial z} = \frac{\partial}{\partial z}\left[K(T) \frac{\partial T}{\partial z}\right] \qquad (11)$$

which differs from the original equation by the convective term $\rho C v(T)\, \partial T/\partial z$. All boundary conditions retain their original form given above, and only $\partial T/\partial x$ is replaced by $\partial T/\partial z$.

The velocity of the receding surface, i.e., $v(T)$ is a highly non-linear function of temperature. A review of the model used to calculate the evaporation losses is given in Ref. [15]. In this model, the surface velocity is highly non-linear function of surface temperature and is given by

$$v(t) = 5.8\times10^{-2} \frac{\alpha\sqrt{A}\, P_v(T_v)}{\rho(T_v)\sqrt{T_v}} \left[0.8 + 0.2\, e^{-t/10\,\tau_c}\right] \text{ cm/sec} \qquad (12)$$

where

α = sticking probability ($\approx$1)
A = atomic mass number of target material
P_v = vapor pressure of target material (Torr)
τ_c = vapor collision frequency (sec^{-1})

Another way of accounting for the receding surface due to vaporization is to solve Eq. (1) without introducing the moving frame of reference. However the temperatures after each time step have to be modified by simple gradient correction term to account for the loss of material in this time step. Thus avoiding the complications of additional term in the heat conduction equation.

LEAVE SPACE FOR
Author's Name Here
Author's Appointment Here

A third way to account for the recession of the surface is to use zone elimination techniques. In this method the first zone gets smaller each time step until its thickness approaches a small value. The first zone is then eliminated and the second zone becomes the first and so on. The advantage of the above two methods over this one is that the total number of zones remains constant, however, each zone is reduced by a factor at each time step. For a matter of illustration the first method is used with the finite difference solution and the second method is used with the finite element representation of the heat conduction equation.

FIRST HEADING HERE
Start text here

3.1 Phase Change

When the temperature of a node reaches the melting temperature of the material T_m, then this node temperature is fixed until all the heat of fusion is absorbed. Then the temperature of this node is allowed to change. During the phase change the material properties of the node is given by a combined value from both solid and liquid properties according to the ratio of the transformation at this time step.

4. FINITE DIFFERENCE SOLUTION

There are several schemes available to express the time-dependent heat-conduction equation in finite difference form ranging from the so-called explicit form to the fully implicit form. Each of these differencing schemes has its advantages and limitations. The finite difference scheme used in solving the above heat conduction equation is based on the modified implicit method of Crank-Nicolson [16]. However, the nature of this particular problem and the highly non-linear boundary condition and the presence of low-order terms in the heat equation may force one to use a smaller value of Δt.

The space is divided into N interval mesh points and the interval spacing may be non-uniform and is chosen such that it

is sufficiently small near the actual surface of the material where evaporation and melting is expected to occur (Fig. 2).

The finite difference representation of Eq. (11) is then given by

$$\rho_J^n C_{P_J}^n \frac{(T_J^n - T_J^{n-1})}{\Delta T}$$

Author's Name Here

$$\frac{1/2\left[(K\nabla T)^n_{J-1/2} + (K\nabla T)^{n-1}_{J-1/2}\right] - 1/2\left[(K\nabla T)^n_{J+1/2} + (K\nabla T)^{n-1}_{J+1/2}\right]}{1/2\left(\Delta X_{j-1} + \Delta X_j\right)}$$

Author's Appointment Here

$$+ \rho_J^n C_{P_J}^n V_J^n \frac{\frac{1}{2}\left[T^n_{J-1} + T^{n-1}_{J-1}\right] - \frac{1}{2}\left[T^n_{J+1} + T^{n-1}_{J+1}\right]}{\left(\Delta X_{j-1} + \Delta x_J\right)} \qquad (13)$$

where

$$(K\nabla T)^n_{J-1/2} = K^n_{J-1/2} \frac{(T^n_{J-1} - T^n_J)}{\Delta X_{J-1}} \qquad (14)$$

$$K^n_{J-1/2} = \begin{cases} \dfrac{K^n_{J-1} + K^n_J}{2} & \text{Arithmatic mean} \\ \dfrac{2K^n_{J-1} K^n_J}{K^n_{J-1} + K^n_J} & \text{Harmonic mean} \end{cases} \qquad (15)$$

$$v^n_J = v^n_{(J=0)} \left(\frac{J_N - J}{J_N}\right) \qquad (16)$$

The governing equation in a tridiagonal system of equations can be written in the form:

$$A_J T^n_{J-1} + B_J T^n_J + C_J T^n_{J+1} = D^{n-1}_J \qquad 1 < J < N-1 \qquad (17)$$

where the coefficients are given by

$$A_J = -\frac{K^n_{J-1/2}}{\Delta x_{j-1}\left(\Delta x_{j-1} + \Delta x_j\right)} - \frac{\rho^n_j C^n_{P_j} V^n_j}{2\left(\Delta x_{j-1} + \Delta x_J\right)} \qquad (18)$$

$$B_j = \frac{\rho_j^n C_{P_j}^n}{\Delta t} + \frac{K_{j-1/2}^n}{\Delta x_{j-1}\left(\Delta x_{j-1} + \Delta x_j\right)} + \frac{K_{j+1/2}^n}{\Delta x_j\left(\Delta x_{j-1} + \Delta x_j\right)} \tag{19}$$

$$C_J = -\frac{K_{J+1/2}^n}{\Delta x_j\left(\Delta x_{j-1} + \Delta x_j\right)} + \frac{\rho_j^n C_{P_j}^n V_j^n}{2\left(\Delta x_{j-1} + \Delta x_j\right)} \tag{20}$$

$$D_J^{n-1} = \frac{\rho_J^n C_{P_J}^n}{\Delta t} T_J^{n-1} + \frac{T_{j-1}^{n-1} K_{J-1/2}^{n-1} - T_j^{n-1} K_{j-1/2}^{n-1}}{\Delta x_{j-1}\left(\Delta x_{j-1} + \Delta x_j\right)}$$

$$- \frac{T_j^{n-1} K_{j+1/2}^{n-1} - T_{j+1}^{n-1} K_{j+1/2}^{n-1}}{\Delta x_j\left(\Delta x_{j-1} + \Delta x_j\right)} + \frac{\rho_j^n C_{P_j}^n V_j^n \left(T_{j-1}^{n-1} - T_{j+1}^{n-1}\right)}{2\left(\Delta x_{j-1} + \Delta x_j\right)} \tag{21}$$

5. BOUNDARY CONDITIONS

Similar equations for surface J=0 and N can be written down based on the boundary conditions of that node. The boundary condition used at the surface J=0 is given by

$$K(T)\,\frac{\partial T}{\partial x}\Big|_{x=0} = q_{net} \tag{22}$$

where

$$q_{net} = q\,(t) - q_v - q_c \tag{23}$$

At the other boundary J=N several boundary conditions can be employed in the code such as radiative, convective, or isolated boundary condition, i.e.,

For a radiative B.C.

$$K(T)\,\frac{\partial T}{\partial x}\Big|_{x=L} = -\varepsilon\sigma\left(T_N^4 - T_a^4\right)\,, \tag{24}$$

For a convective B.C.

$$K(T)\,\frac{\partial T}{\partial x}\Big|_{x=L} = h\left(T_N - T_c\right) \tag{25}$$

where h is the heat transfer coefficient of the fluid used to cool the wall and T_c is the coolant temperature.

For an isolated B.C.

$$K(T) \frac{\partial T}{\partial x} \Big|_{x=L} = 0 \tag{26}$$

The governing equation and the coefficients for the tridiagonal matrix can similarly and easily be obtained for each boundary condition.

An implicit alternating direction method suggested by Peaceman and Rachford [17] is used to solve the two-dimensional problem. This method is only valid for linear equations, but may be used here by transforming the nonlinear system (material properties, boundary conditions and zone thicknesses may be temperature or time-dependent) into a quasi-linear system in which the nonlinear coefficients are frequently reevaluated.

6. FINITE ELEMENT SOLUTION

Using variational calculus the differential Eq. (1) and the boundary and initial conditions are transformed into a functional I defined as

$$I = \int_v \left[\frac{1}{2} K\left(\frac{\partial T}{\partial x}\right)^2 - \left(\rho C_p \frac{\partial T}{\partial t}\right)T\right]dV + \int_{s1} q_1 T ds + \int_{s2} q_2 T ds \tag{27}$$

The solution is achieved by minimizing the above equation with respect to temperature, which yields

$$[K] \{T\} + [C] \frac{\partial \{T\}}{\partial t} + \{F\} = 0 , \tag{28}$$

where

$[K]$ = global stiffness matrix
$[C]$ = global capacitance matrix
$\{T\}$ = global temperature vector
$\{F\}$ = global force vector.

The time derivative of Eq. (28) is approximated by using a central difference scheme such that

$$[A] \{T\}^n = [B] \{T\}^{n-1} - \{F\}^{n-1} , \tag{29}$$

where

$$[A] = \left[[K] + \frac{2}{\Delta t} [C]\right] \tag{30}$$

$$[B] = \left[\frac{2}{\Delta t}[C] - [K]\right] \tag{31}$$

For a one-dimensional linear element and for the same geometry (Fig. 2) and the same boundary and initial conditions, the matrices are defined as

$$[K^J] = \frac{(K_J + K_{J+1})}{2\ \Delta x_J} \begin{bmatrix} 1 & -1 \\ -1 & 1 \end{bmatrix} \tag{32}$$

and

$$[C^J] = \frac{(\rho_J C_{P_J} \Delta x_J + \rho_{J+1} C_{P_{J+1}} \Delta x_{J+1})}{12} \begin{bmatrix} 2 & 1 \\ 1 & 2 \end{bmatrix} \tag{33}$$

for the consistent formulations, or

$$[C^J] = \frac{(\rho_J C_{P_J} \Delta x_J + \rho_{J+1} C_{P_{J+1}} \Delta x_{J+1})}{4} \begin{bmatrix} 1 & 0 \\ 0 & 1 \end{bmatrix} \tag{34}$$

for the lumped formulations.

The value of the force vector is dependent on the boundary conditions imposed on that particular element. For example, the force vector for the first element containing nodes 1 and 2 is

$$\{F\} = \begin{Bmatrix} q_{net} \\ 0 \end{Bmatrix} \tag{35}$$

where q_{net} is given by Eq. (23). The value of the force vector of the last element is also dependent on the boundary condition used for that element. All the other internal force vectors are equal zeros for this particular problem, unless there is a specified volumetric heat generation rate.

After each time step the temperatures throughout the target have to be corrected for the loss of material at this time step. The corrected temperature for node j, T_j^c, is simply given by

$$T_j^c = T_j^n - \frac{\partial T_j^n}{\partial x_j} \delta x_j \tag{36}$$

where δx_j is the reduction in thickness of zone j due to the evaporation.

7. APPLICATIONS

7.1 High Energy Deposition on Target Materials

Disruptions in magnetic fusion reactors lead to high energy deposition for short times on in-vessel components. Melting and evaporation may then occur. An accurate prediction of these quantities require the solution of two moving boundaries discussed above. Table 1 shows the thermal response and the resulting vaporization and melt layer thicknesses calculated by both finite difference and finite element methods for two candidate materials, vanadium and stainless steel. The calculation is done for an energy density of 1000 J/cm^2 deposited in two different times of 10 and 50 ms. The agreement between the finite difference and the finite element is very good. Vanadium yields less vaporization than steel because of its lower vapor pressure. It can also be seen that the energy expaned in vaporization is much more than that lost due to radiation. Higher energy lost to vaporization means less energy available for conduction to cause melting [20-21]. Longer deposition times allow more time for the energy to be conducted away from the surface and hence less energy to produce vaporization but may cause more melting.

7.2 Vaporization of Small Spherical Pellets

Another application for the solution of the two moving boundaries problem is to calculate the lifetime of spherical metallic pellets, injected into the edge of a plasma "scrape-off region" to be vaporized and redeposited for coating purposes. The heat flux in this particular application is not extremely high ($\approx$2-4 MW/m^2) thus the pellet vaporization can be approximated and treated as a heat transfer problem rather than a complicated hydrodynamic problem [23].

The heat conduction equation in spherical coordinates is given by

$$\rho C_p \frac{\partial T}{\partial t} = K \frac{d^2T}{dr^2} + \frac{2K}{r} \frac{dT}{dr} . \qquad (37)$$

The instantaneous radius of the injected pellet can be given as

$$r(t) = R_o - \int_o^t V(T)\, dt \qquad (38)$$

where

R_o = pellet radius at t = 0
$V(T)$ = velocity of the eroding surface (Eq. 12).

The boundary condition on the pellet surface can also be given by Eq. (7), while the boundary condition at the origin is similar to that of Eq. (26).

The solution methods and procedure is similar to the one-dimensional Cartizian coordinates and will not be discussed in detail here. The pellets are dropped in a constant heat flux region where their temperature starts rising to cause melting and vaporization. The lifetime (time for complete vaporization) of the pellet is determined when the radius is reduced to less than 0.5% of its initial value as a result of the continuous erosion of surface material, then the calculation is stopped. The heat flux is assumed uniform on the whole surface of the pellet.

As an example the time for complete melting and the lifetime of the pellet for both vanadium and steel is shown in Table 2. Two heat fluxes of 2 MW/m^2 and 4 MW/m^2 are considered. The initial pellet radii is taken to be 100 μ and the emissivity of both materials are assumed to be one. The pellet lifetime is linearly proportional to the pellet radius. The calculation shown is done by the finite difference method. The time for complete melting is much shorter than the lifetime. An interesting point to mention that most of the energy supplied to the pellet is lost in radiation in contrast to the previous application where most of the energy lost in vaporization. This is mainly because of the geometrical configuration of this particular problem. As a result any decrease in emissivity of the material will substantially reduce the lifetime. This is because lower emissivities means less energy lost by radiation and consequently higher surface temperatures which result in higher evaporation.

7.3 Electron or Ion Beam Interaction with Materials

Simulation experiments of high energy ion or electron beam interaction with materials and the resulting thermal effects is modeled by solving the time dependent heat conduction equation in axially symmetric cylinderical coordinates (r,z). Where r is the radial distance measured from the center of the beam and z is the coordinate normal to the sample surface with origin at the surface. This equation is given by [20]

$$\rho C \frac{\partial T}{\partial t} = \frac{1}{r} \frac{\partial}{\partial r} \left(Kr \frac{\partial T}{\partial r} \right) + \frac{\partial}{\partial z} \left(K \frac{\partial T}{\partial z} \right) + Q\,(r,z,t) \qquad (39)$$

Equation (39) is solved using the same procedure discussed above except it is done in two dimensions. The boundary con-

Table 1
Thermal Response of Vanadium and Stainless Steel
by Finite Difference (FD) and Finite Element (FE) Methods
Energy Deposited 1000 J/cm^2, Initial Wall Temperature 300°C

Parameters	10 ms Deposition Time				50 ms Deposition Time			
	Vanadium		Stainless Steel		Vanadium		Stainless Steel	
	FD	FE	FD	FE	FD	FE	FD	FE
Maximum Surface Temp. (°K)	3800.1	3801.1	3287.72	3287.95	3248	3248.6	2864.6	2865.45
Vaporization Thickness (μ)	78.89	79.25	157.3	157.4	14.82	15.14	81.40	81.56
Melting Thickness (μ)	286.4	286.7	204	204	432.9	448.8	364.85	365.26
% Energy in Vaporization	45.41	45.61	66.37	66.39	8.53	8.72	37.13	37.20
% Energy in Radiation	.151	.152	0.085	0.085	3.25	3.27	2.26	2.26

Table 2
Finite Difference Solution for Spherical Pellet's Lifetime Calculations
100 μ Pellet Radii, 300°C Initial Temperature

Heat Flux	2 MW/m^2		4 MW/m^2	
Material / Parameter	Vanadium	Stainless Steel	Vanadium	Stainless Steel
Maximum Temperature (°K)	2405	2142	2650	2270
Time for Complete Melting (ms)	28	24	13.4	11.7
Time for Complete Vaporization (s)	36	6.1	4.4	2.0
% Energy in Vaporization	7	41	31	63
% Energy in Radiation	93	59	69	37

ditions are also similar to the one-dimensional case with the input heat flux may vary radially along the surface of the target, i.e.,

$$q(r,t) = -K(T_v)\frac{\partial T}{\partial z} + \rho(T_v)V(r,T)L_v + \sigma\varepsilon(T_v^4 - T_a^4) \qquad (40)$$

It is found that the vaporization and melting of the target is strongly depends on the characteristics of the beam spatial distribution, beam diameter, and on the time variation of the beam power [20]. As an example the maximum surface temperature rise (i.e., at the center of the beam) is shown in Fig. (3) for both copper and steel for an energy density of 800 J/cm^2 deposited in 50 ms [20]. The temperature rise is shown for different flat beam diameters. For beam diameters >1 mm the steel surface temperature is much higher than that for copper and the steel stays in the liquid phase for about 100 ms. Lateral conduction along the beam surface is very important for smaller beam diameters as it can be seen for the copper case where it does not melt for beam diameters around 1 mm compared to the 3 mm beam diameter case, where about 360 microns of the copper is predicted to melt.

8. CONCLUSIONS

The time dependent heat conduction equation is solved with two moving boundaries in different coordinate systems subject to various boundary conditions. The first moving boundary is the receding surface as a result of evaporation of surface materials. The second moving boundary is the melt-solid interface due to the change of phase in the material. The boundary conditions include surface heat flux, energy to vaporization, radiation from the surfaces and phase change. Both finite difference and finite element methods are used in the solution and show good agreement. The solution developed in different coordinate systems has several important applications in space, fusion reactors, and weapons research, involving high energy deposition and interaction of different radiation with matter.

9. REFERENCES

[1] OZSISIK, M. N., Heat Conduction (Wiley-Interscience, New York, 1980).

[2] MUEHLBAUER, J. C. and SUNDERLAND, J. E., Applied Mechanics Reviews 18 (1965) 951.

[3] OKKENDON, J. R. and HODGKINS, W. R., ed., Moving Boundary Problems in Heat Flow and Diffusion (Clarendon Press, Oxford, 1975).

[4] WILSON, D., SOLOMON, A., BOGGS, P., ed., Moving Boundary Problems (Academic Press, New York, 1978).

[5] READY, J. F., Appl. Phys. Letters 3 (1963) 11.

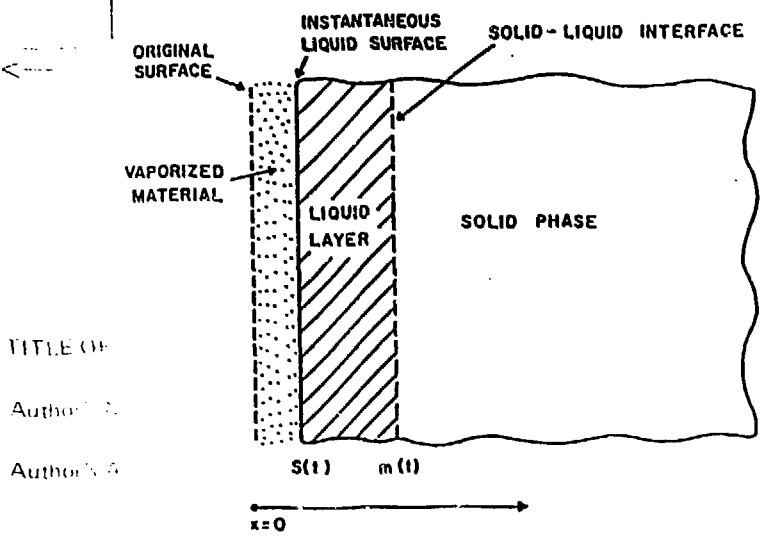

Fig. 1 Schematic representation of solid- liquid-vapor interfaces.

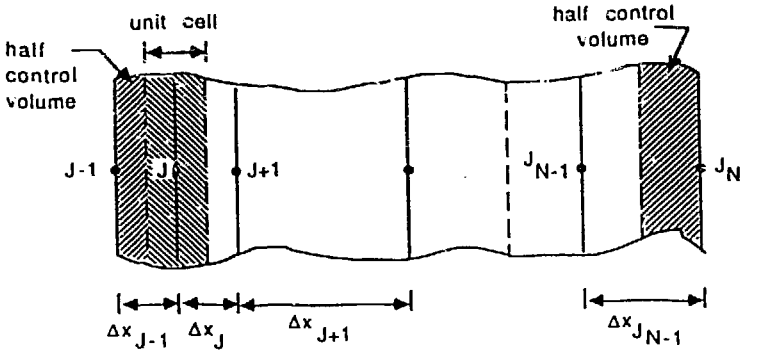

Fig. 2 One-dimensional finite difference model with non-uniform mesh.

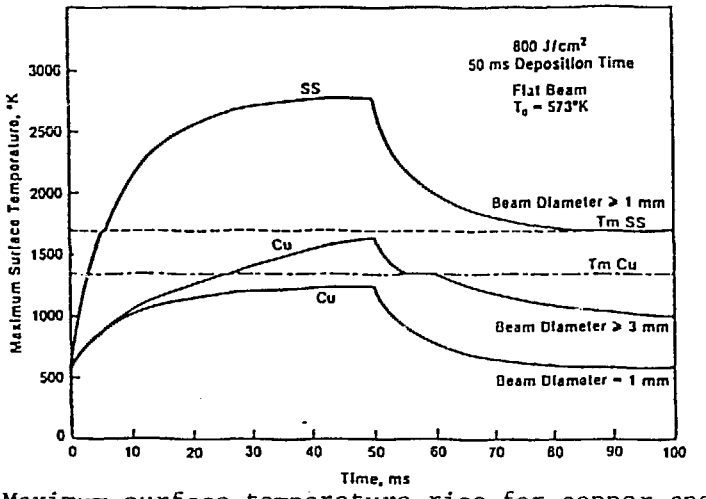

Fig. 3 Maximum surface temperature rise for copper and stainless steel.

[6] READY, J. F., J. Appl. Phys. 36 (1965) 2.
[7] ANDREWS, J. G. and ATTHEY, D. R., J. Inst. Maths. Appl. 15 (1975) 59.
[8] LOEBEL, L. L. and WOLFER, W. G., University of Wisconsin Report UWFDM-370 (1980).
[9] BEHRISCH, R., Nuclear Fusion 12 (1972) 695.
[10] OSADIN, B. A. and SHAPOVALOV, G. I., Teplofizika Vysokikh Temp. 10 (9172) 361.
[11] GOLODENKO, N. N. and KUZ'MICHEV, V. M., Teplofizika Vysokikh Temp. 10 (1972) 1126.
[12] MERRILL, B. J., in 9th Symp. on Engrg. Problems of Fusion Research, Chicago, Oct. 1981.
[13] FILLO, J. A. and MAKOWITZ, H., ibid.
[14] BOWERS, D. A. and HAINES, J. R., J. Nucl. Mater. 103&104 (1981) 81.
[15] HASSANEIN, A. M., KULCINSKI, G. L., and WOLFER, W. G., J. Nucl. Mater. 103&104 (1981) 321.
[16] CRANK, J. and NICHOLSON, P., Proc. Camb. Phil. Soc. 43 (1947) 50.
[17] PEACEMAN, D. W. and RACHFORD, H. H., J. Soc. Indust. Appl. Math. 3 (1965) 28.
[18] HASSANEIN, A. M., KULCINSKI, G. L., and WOLFER, W. G., Nuclear Eng. and Design/Fusion, Vol. 1 No. 3, July 1984 (307-324).
[19] HASSANEIN, A. M. and KULCINSKI, G. L., J. Heat Transfer Vol. 106, August 1984 (486-490).
[20] HASSANEIN, A. M., J. Nucl. Mat. 122&123 (1984) 1453-1458.
[21] HASSANEIN, A. M., J. Nucl. Mat. 122&123 (1984) 1459-1465.
[22] HASSANEIN, A. M., ATTAYA, H. M., and KULCINSKI, G. L., J. Nucl. Mat. 141-143 (1986) 221-225.
[23] EHST, D. A., et al., "Tokamak Power Systems Studies," Argonne National Laboratory Report ANL/FPP/86-1, March 1987.